Optical properties of highly oriented nanostructured CuI (111) thin films

P. V. C. LUHANGA[a*], C. MUIVA[b], S. H. COETZEE[c,d], K. MAABONG[a], L. TIEDT[e], P. MONOWE[a]
[a]*Department of Physics, University of Botswana, Private Bag 0022, Gaborone, Botswana*
[b]*Department of Physics, Botswana International University of Science and Technology, Private Bag 16, Palapye, Botswana*
[c]*Botswana Institute for Technology, Research and Innovation (BITRI), Private Bag 0082, Gaborone, Botswana*
[d]*African Materials Science and Engineering Network (AMSEN)*
[e]*Laboratory for Electron Microscopy, North West University, Potchefstroom Campus, Private Bag X6001, Potchefstroom, 2520 South Africa*

Transparent nanostructured copper(I) iodide (CuI) thin films of varying thicknesses were deposited by thermal evaporation of pre-melt quenched CuI powders and their structural and optical properties are reported. X-ray diffraction characterization identifies γ-CuI and suggests that the films are monocrystalline in nature showing high crystallographic orientation along CuI (111). SEM studies reveal spherical granules growing in size with increasing film thickness. Thinner films were characterised by high dislocation densities. Optical studies revealed a red shift in the absorption edge and decreased optical band gap energies with film thickness.

(Received August 7, 2015; accepted September 29, 2016)

Keywords: CuI, Nanostructures, Thin films, Evaporation, Optical properties

1. Introduction

Cuprous Iodide (CuI) belongs to the I–VII semiconductors with Zinc-blende structure. Recently, CuI has drawn a great deal of attention, as it is a versatile material for optoelectronic applications. The versatility of this inorganic semiconducting material lies in its coordination chemistry which allows it to link readily with many inorganic and organic ligands [1]. CuI is one of the few p-type wide band gap materials which are transparent in the visible range. Nanostructured semiconductors are taking a centre stage in the continuous miniaturisation of optoelectronic devices. In addition, nanostructured materials show a large surface area and size dependent quantum effects that have enhanced properties as compared to the bulk. Nanostructured CuI has shown feasible applications in catalysis, drug delivery systems, buffer layer in $CuInX_2$ (X=S, Se and Te) based solar cells, photonics, piezoelectric transducers, solid state electrolytes in dye sensitised solar cells, top emission organic light emitting diodes (TEOLEDs) and dielectric devices [1-3].

CuI is found in three crystalline phase of α, β and γ. The first form is a cubic and it is formed at a temperature of 392 ^oC while the β phase is hexagonal and it is stable between temperatures of 392 ^oC and 350 ^oC. The γ phase with zinc blende cubic structure appears at temperature below 350 ^oC. In CuI the topmost valence bands (Γ 15,2 and Γ 12,1) are obtained from the 3d states of Cu and 5p states of I. The energy difference of the Γ 15,2 and Γ12,1 valleys at the Γ point in the Brillion zone give rise to a direct optical band gap usually reported as 3.1 eV [4, 5].

Several routes have been used to deposit nanostructured CuI thin films. A chemical route was recently reported by Johan *et al* [6]. Others include solvothermal [1], magnetron sputtering [7], spray pyrolysis technique [8], pulsed laser [9] and iodation of porous copper [10]. Comparative studies on p-type CuI grown on glass and copper substrate by successive ionic layer adsorption and reaction (SILAR) method have been reported [11]. Of these methods, sol–gel routes can be particularly simple alternatives to fabricate thin films containing copper halide nanoparticles. However, preparing the sol-gel precursors in aqueous form can readily shift the oxidation states (Cu^{2+}/Cu^{+}) equilibrium mainly towards Cu^{2+}, thus making it difficult to prepare exclusively CuI. These drawbacks can be overcome through a more pure route such as vacuum thermal evaporation. There seems to be few reports on deposition of nanocrystalline CuI by thermal evaporation. Shuo *et al* [12] have reported synthesis of copper nanowires from CuI thin films synthesised through thermal evaporation. In this study, we report the synthesis and characterization of CuI thin films deposited on glass by thermal evaporation of pre-melt quenched bulk CuI.

2. Experimental details

Stoichiometric quantities of Cu and Iodine powders were weighed. The samples were then sealed in single crystal silica ampoules. The ampoules were evacuated to a pressure of 10^{-5} Torr and backfilled with Argon gas to a pressure of 10^{-3} Torr. The ampoules were then sealed off

under vacuum by utilizing an acetylene torch flame. The ampoules were heated in a ramping horizontal tube furnace for 12 hours at a temperature of 700°C and rapidly transferred to Ethanol Liquid Nitrogen slush for quenching. Copper and Iodine melt at 1083.4 °C and 113.5°C, respectively [13]. The melting point of γ-CuI is 602°C [14]. Thus the temperature of 700°C was chosen to allow Iodine to melt and diffuse into the Cu forming CuI. Thin films of CuI were then fabricated by evaporating the pre-melt quenched CuI onto micro-slides in a high vacuum chamber operating at a base pressure of 10^{-5} Torr. Electron microscopy investigation was conducted on a Fei Quanta 250 FEG. The structural morphology was investigated using a Philips XL 1710 XRD system with characteristic Cu-Ka 1 with a wavelength of 1.54056 Å. The transmittance (T) and reflectance (R) spectra of each sample were measured using a CARY 500 UV/VIS/NIR double beam spectrophotometer. The thickness of the films was obtained using a Tencor P15 KLA Profiler with an accuracy of 0.1 Å. The samples with thickness (d) 30.3 nm, 36.6 nm and 57.9 nm were labeled as CuI 1, CuI 2 and CuI 3 respectively.

3. Results and discussion

Fig. 1 shows the XRD bitmaps of CuI 3 compared against that of the uncoated glass slide. It can be inferred that the growth was highly oriented towards a single crystallographic growth along the (111) axis perpendicular to the substrate surface. The single peak was indexed to the face centred-cubic (fcc) structure of γ-CuI, space group F-43 m (216), JCPDS card No. 06-0246. Peak broadening is indicated by the angular width of the peaks at full width at half maximum (FWHM) and is known to be inversely proportional to the crystallite size [15]. The broadening of the XRD peak indicated that the crystallites were nanosized.

The mean crystallite size (C) was calculated from the FWHM (β), Bragg's angle (θ) and the wavelength (λ) of the X-ray radiation using the Debye-Scherrer equation 1 [16];

$$C = \frac{0.9\lambda}{\beta Cos\theta} \quad (1)$$

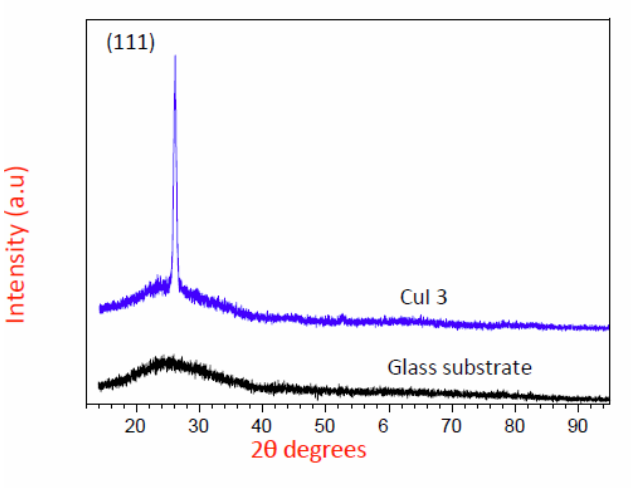

Fig. 1. XRD bitmap of CuI 3 thin film and the glass substrate

Fig. 2 shows the SEM images of the samples. In all the samples nanocrystalline spherical granules spread randomly over the surface were observed. EDS analysis showed that the samples had stoichiometric compositions averaging 50.9 and 49.1 at.% for copper and iodine, respectively. The average grains size (D) were estimated from the SEM scale and obtained as 50.3, 68.4, 97.3 nm for CuI 1, CuI 2 and Cu 3, respectively as indicated in Table 1. The crystallite size for CuI 3 was obtained as 45 nm. The dislocation density (δ) of the grains in the CuI films is related to the grain size (D) through Eq. 2 [17];

$$\delta = 1/D^2 \quad (2)$$

The deduced values of δ are entered in Table 1. These results and SEM images show that there are large densities (in the order of 10^{10} cm^{-2}) of inter granular dislocations meaning that some portion of XRD beam is reflected by the substrate, which collaborates with the low crystallinity in the thinner films.

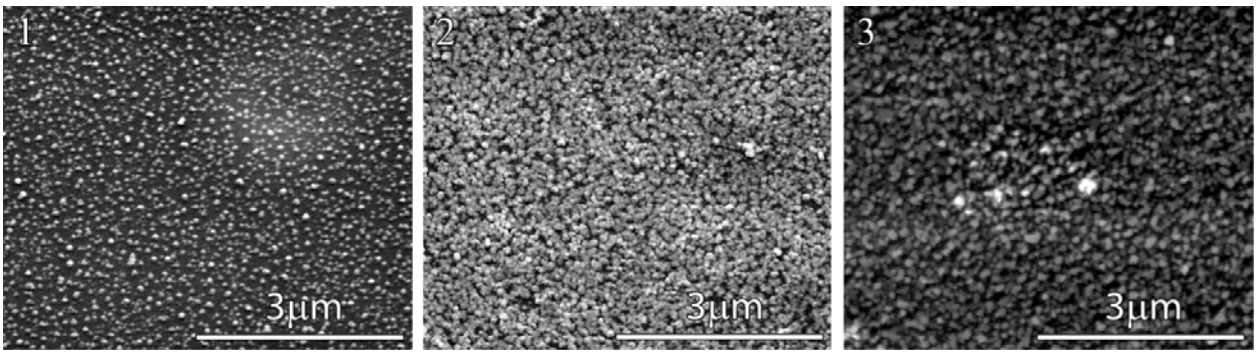

Fig. 2: SEM images of the CuI thin films

It was observed that the grains size increased with increased film thickness. This indicates that the film thickness contributes to the improvement in crystallinity. It can be inferred from the dimensions that the grains were

almost semispherical (D/d ≈ 2) with the flat base in contact with the substrate. In the process of deposition of a film via vapor methods, a film does not build uniformly (one atomic layer after another) on the substrate surface at the same time. Isolated nuclei are formed, consisting initially of relatively small numbers of atoms. As the deposition continues, these nuclei grow and form isolated grains or crystallites. The crystallographic orientation in the plane of the film of these crystallites is random in the case of amorphous substrates. At this stage the film is often referred to as an "island film". As more material is deposited new nuclei may be formed or existing ones grow larger. Eventually the islands touch and this is the onset of conduction. For CuI the film is highly oriented towards (111) meaning that growth towards this crystallographic direction has the lowest surface energy [18, 19]. This favors growth of existing CuI nuclei over formation of new ones which contributes to the observed increased grain size with film thickness.

Fig. 3 shows the spectral dependence of the normal transmittance and reflectance of the as-deposited CuI samples of different thickness. The transmittance in the maximum solar irradiance wavelength (550 nm) of the visible spectrum was above 70 % for all the samples. This result reveals that the obtained samples will provide a suitable window for optical device applications. In the absorption region, the transmittance decreases rapidly due to fundamental absorption related to excitation of carriers across the energy gap. The transmittance seems to decrease in the vicinity of the excitation energy of CuI pointing to a cut off wavelength of around 400 nm. There was a slight red shift in the absorption edge with increasing film thickness. The less transmittance in thicker films is attributed to increased photon absorption due to increased path lengths in the thicker films. Light is absorbed as it passes through materials and the attenuation is governed by the Beer Lambert's law; $I(x) = I_o e^{-\alpha x}$ [20] where I_o is the incident intensity, I is the transmitted intensity, α is the absorption coefficient and x is the thickness of the material. It was observed that the thinner films generally showed higher transmittances and sharper absorption edges. The less sharp absorption edge in the thicker film is due to the fact that for bigger grain sizes the scattered radiation became remarkable due to the surface roughness [21].

The optical properties of a material are described by how certain characteristics of light change when it is propagated through it. Absorption coefficient (α) is one of the physical properties that control light propagation through a media. The absorption coefficient (α) transmittance (T) and reflectance (R) are related to film thickness (d) through Eq. 3 [22];

$$\alpha = (1/d)ln[(1-R)^2/T] \quad (3)$$

The extinction coefficient (k) is inversely proportional to the distance which a photon travels before it is absorbed. k is related to α through the relation given in Eq. 4 [23];

$$k = \alpha\lambda/4\pi \quad (4)$$

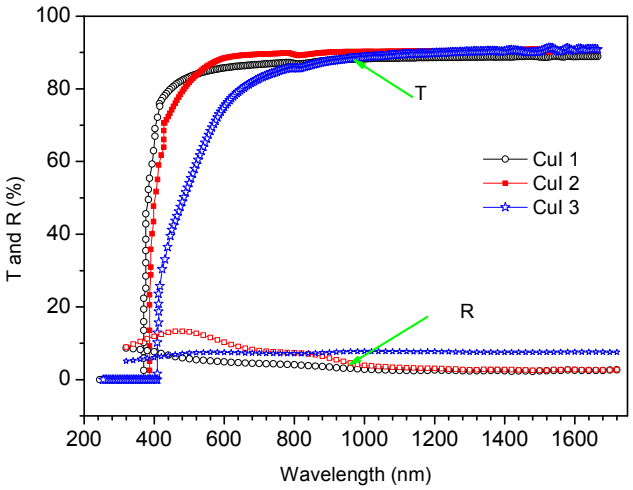

Fig. 3. Transmittance (T) and Reflectance (R) spectra of the CuI samples

Fig. 4 shows the spectral dispersion of the extinction coefficient (k) of the CuI thin films. The samples show low absorption coefficient in the visible range. It was further observed that the absorption coefficient increases rapidly in the vicinity of the absorption edge, which indicates that the CuI films have a good homogeneity in the shape and grain size [24] as also observed under SEM.

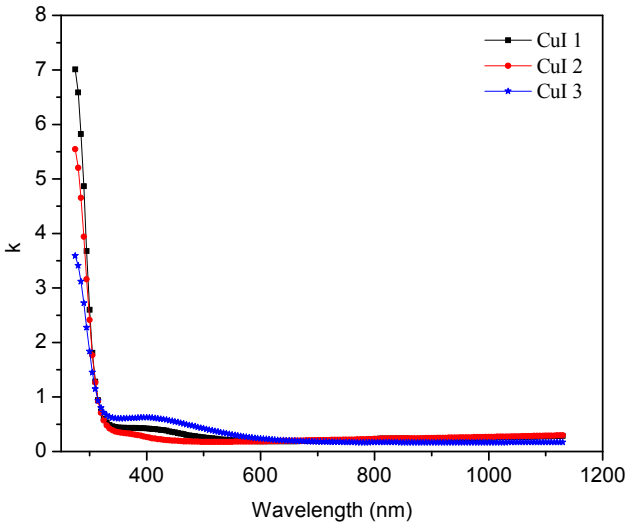

Fig. 4: Extinction coefficient (k) of the CuI thin films

An attempt was made to analyse the observed absorption spectrum of the systems under study on the basis of Tauc's model [25] which is based on Eq. 5;

$$(\alpha hv) = (B - E_g)^n \quad (5)$$

where B is a constant. The superscript, n in the Tauc's expression (Eq. 5) is associated with the nature of photon induced electronic excitations across the energy gap.

Specifically, n is 1/2, 3/2, 2 and 3 for direct-allowed, direct-forbidden, indirect-allowed, and indirect-forbidden respectively. CuI is known to have an allowed direct band gap [11, 26], therefore n = 1/2 was used in calculations in this work. Plots of $(\alpha h\nu)^2$ as a function of photon energy ($h\nu$) (Fig. 5) reveal a linear portion near the absorption edge. E_g was determined by extrapolation of this linear region to zero where the factor $(\alpha h\nu)^2 \rightarrow 0$, as $\alpha \rightarrow 0$ in the transparency region.

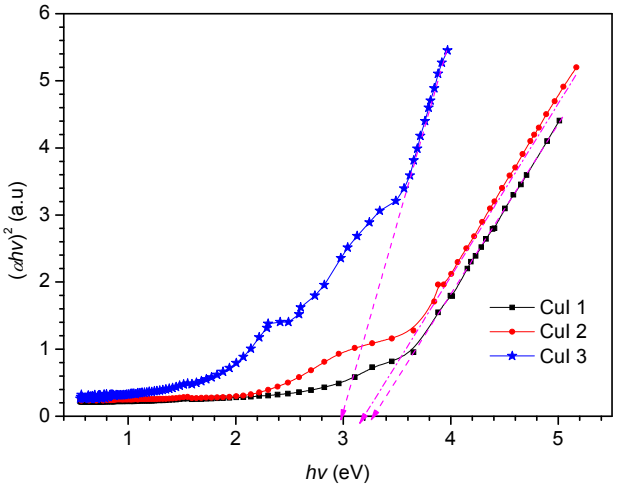

Fig. 5: Taucs's plot for obtaining the optical band gap

Values of E_g were evaluated and listed in Table 1. The variation of E_g with film thickness is shown in Fig. 6. The obtained E_g values were found to decrease with film thickness which is consistent with the observed red shift in the transmission spectra. The observed decrease in band gap values with film thickness may be attributed to the enhancement in the crystalline morphology of the films and increase of grain size [27]. Optical band gap is sensitive to the microstructure of a material. The decreased bandgap in thicker films may be related to reduction in stacking faults, lattice defects and increased grain size as film thickness increased pointing to enhanced film crystallinity [28]. According to Shim et al., [29], this trend could be due to the decrease of strain at the interface between CuI film and glass substrate brought by increased film thickness and larger grains [30].

However, the E_g values obtained for CuI 1 and CuI 2 are higher (+ 0.2 and 0.1 eV respectively) than the reported [31] value of 3.1 eV. It is worth noting that semiconductor nanoparticles are known to have unique size-dependent physical characteristics. Nanoscale semiconductor particles are associated with increased band gap values due to quantum confinement [30, 32] which may be the case for this study. The ionic radius of Cu and iodine is 0.074 nm and 0.206 nm respectively. The structural implication is that squeezing iodide into the tightly packed (111) planes during growth can lead to a high probability of formation of iodide vacancies [1].

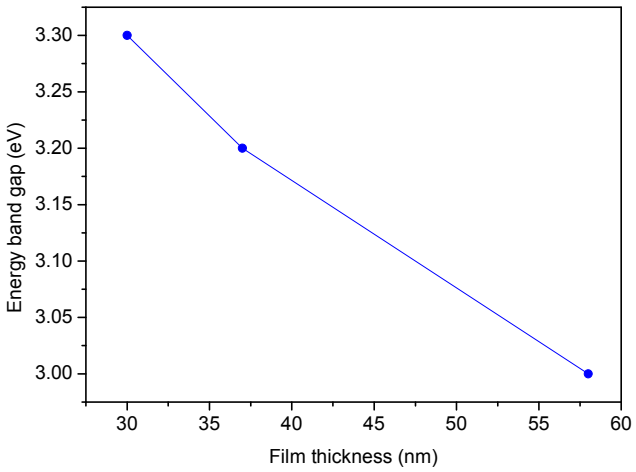

Fig. 6: Variation of Energy band gap with film thickness.

Table 1: Values of film thickness (d), grain size (D), dislocation density (δ) and energy band gap (E_g)

	d (nm)	D (nm)	δ x 10^{10} cm^{-2}	E_g (eV)
CuI 1	30.3	56.8	3.10	3.3
CuI 2	36.6	68.4	2.14	3.2
CuI 3	57.9	97.3	1.06	3.0

4. Conclusions

Nanostructured CuI thin films were deposited by thermal evaporation of the melt quenched bulk samples. XRD studies revealed growth of highly oriented (111) γ - CuI films. In all the samples nanocrystalline spherical granules spread randomly over the surface were observed. The grain sizes increased with increased film thickness. There was a red shift in the absorption edge with film thickness which was consistent with decreased band gap values. The decreased bandgap in thicker films may be related to reduction in stacking faults, lattice defects and increased grain size as film thickness increased pointing to enhanced film crystallinity.

Acknowledgements

The authors would like to thank the University of Botswana Research Committee (URC) for financial support through research grant R-1068 .

References

[1] Z. Zheng, A. Liu, S. Wang, B. Huang, K. W. Wong, X. Zhang, S. K. Hark, W. M. Lau, J. Mater. Chem. **18,** 852 (2008).

[2] A. R. Zainun, M. H. Mamat, U. M. Noor, M. Rusop, Mater. Sci. Eng., **17,** 012009 (2011).
[3] P. M. Sirimanne, M. Rusop, T. Shirata, T. Soga, T. Jimbo, Mater. Chem. Phys. **80**, 461 (2003).
[4] B. Bouhafs, H. Heireche, W. Sekkal, H. Aourag, M. Certier, Phys. Lett. A **240,** 257 (1998).
[5] W. Sekkal, A. Zaoui, Physica B, **315,** 201 (2002).
[6] M. R. Johan, K. Si-Wen, N. Hawari, N. A. K. Aznan, Int. J. Electrochem. Sci., **7,** 4942 (2012).
[7] T. Tanaka, K. Kawabata, M. Hirose, Thin Solid Films **179**, 281 (1996).
[8] M. N. Amalina, A. R. Zainun, N. A. Rasheid, M. Rusop, Proc. ICSE 2012, Kuala Lumpur, Malaysia (2012).
[9] P. M. Sirimane, M. Rusop, T. Shirata, T. Soga, T. Jimbo, Chem. Phys. Letters **366,** 485 (2002).
[10] Y. Yang , X. Li, B. Zha, H. Chen , X. Bao, Chem. Phys. Letters., **387**, 400 (2004).
[11] S. L. Dhere, S. S. Latthe, C. Kappenstein, S.K. Mukherjee, A. Venkateswara Rao, Appl. Surf. Sci., **256**, 3967 (2010).
[12] S. Shi, J. Sun, J. Zhang, Y. Cao, Physica B, **362**, 231 (2005).
[13] W. Benson, J.W. Harris, H. Stocker, H. Holger, Ed. H. Stocker, Handbook of Physics, Springer-Verlag, New York, USA, 2002.
[14] T.B Massalski, Eds. H. Okamoto and T. Massalaski., Binary Alloy Phase Diagrams, Amer. Soc. Metals, Ohio, USA, 1990.
[15] Z.Q. Li, C.J. Lu, Z.P. Xia, Y. Zhou, Z. Luo, Carbon **45,** 1686 (2007).
[16] B.D. Cullity, S.R. Stock, Elements of X-Ray Diffraction, Prentice-Hall, New York, 2001.
[17] S. Subramanian, D. P. Padiyan, Mater. Chem. Phys. **107**, 392 (2008).
[18] A. C. Tickle.Thin film transistors. John Wiley and Sons, New York. USA, 1969.
[19] N. Fujimura, T. Nishihara, S. Goto, J.g Xu, T. Ito, J. Cryst. Growth, **130** 269 (1993).
[20] D.L. Chung, Functional Materials, World Scientific Publishing, London, UK, 2010.
[21] S.A. Mahmoud, A.A. Akl, H. Kamal, K. Abdel-Hady, Physica B, **311** 366 (2002).
[22] G. Lucovsky, Phys. Rev. B, **15,** 572 (1970).
[23] J. I. Pankove, Optical Processes in Semiconductors, Prentice-Hall, NJ, USA, 1971.
[24] Y. You-hua, L. Ying-chun, F. Ling, L. Zhi-chao, L. Zheng-bang, Z. Shao-xiong, Trans. Nonferrous Met. Soc. China, **21**, 359 (2011).
[25] J. Tauc, Amorphous and Liquid Semiconductors, Plenum Press, New York, USA, 1974.
[26] B.R. Sankapal , E. Goncalves, A. Ennaoui, M.Ch. Lux-Steiner, Thin Solid Films, **451–452,** 128 (2004).
[27] M. N. Amalina, N. A. Rasheid, M. Rusop, Journal of Nanomaterials, **2012,** 1 (2012).
[28] N. E. Makori, I. A. Amatalo, P. M. Karimi, W. K. Njoroge, American Journal of Condensed Matter Physics, **4,** 87 (2014).
[29] E. S. Shim, H. S. Kang, J. S. Kang, J. H. Kim, S. Y. Lee, Appl. Surf. Sci., **186**, 474 (2002).
[30] M. Öztas, M. Bedir, Thin Solid Films **516,** 1703 (2008).
[31] S.A. Mohamed, A.A. Al-Ghamdi, G.D. Sharma, M.K. El Mansy, J. Adv. Res., **5,** 79 (2014).
[32] H. Wang, P. Fang, Z. Chen, S. Wang, Appl. Surf. Sci. **253,** 849 (2007).

*Corresponding author: luhangap@mopipi.ub.bw